Observed limiting cases of horizontal field coherence and array performance in a time-varying internal wavefield

Jon M. Collis
Boston University, 110 Cummington St., Boston, Massachusetts 02215
jcollis@bu.edu

Timothy F. Duda and James F. Lynch
Applied Ocean Physics and Engineering Department, MS 11, Woods Hole Oceanographic Institution, Woods Hole, Massachusetts 02543
tduda@whoi.edu, jlynch@whoi@edu

Harry A. DeFerrari
University of Miami, Miami, Florida 33149
hdeferrari@rsmas.miami.edu

Abstract: Using a moored source and horizontal/vertical line array combination, horizontal coherence properties of high signal to noise ratio ($\geq$20 dB) 100–1600 Hz signals have been measured. Internal waves in the area of the measurement created moving episodic sound-speed anomaly structures, influencing coherence length. Measured horizontal coherence scales for 100 Hz ranged from 5 to 20 acoustic wavelengths, and were inversely related to the sound-speed anomaly strength. Horizontal field properties were compared with fields computed using modal decompositions of the vertical signals. The comparison allows azimuthal field coherence properties to be studied apart from normal-mode interference effects.

PACS numbers: 43.30.Re, 43.30.Bp, 43.30.Ft [DKW]
Date Received: February 26, 2008 **Date Accepted:** May 14, 2008

1. Introduction

To study acoustic fields and their coherence over significant distances, the research community has recently taken steps to enable routine use of co-located horizontal and vertical line arrays (HLAs and VLAs), typically arranged in the shape of the Roman letter L, with the horizontal section on the seafloor.[1] To analyze horizontal coherence we introduce a procedure tailored to oblique incidence on the HLA. Mode interference that occurs over range will introduce incident-angle dependent signal variability along the HLA which we seek to separate from transverse signal decorrelation effects, associated with azimuthally varying propagation (i.e., without cylindrical symmetry). The procedure uses joint analysis of the vertical and horizontal line array receptions. Impulsive mode arrivals (including mode multipath) from fixed sources are estimated using the vertical array. Coherence of measured waveforms of oblique incidence on the horizontal array is compared with that of signals having spatially independent normal mode amplitudes and wave numbers (the fixed-mode field) synthesized using the vertical array modal arrivals. The comparison discloses azimuthal (relative to the source) decorrelation effects without the restriction of having broadside HLA signal incidence. Array gain degradation results for the measured and synthetic fields are also presented, providing additional estimates of field coherence. The results show two behaviors, one where the azimuthal effect is significant enough to be measureable, and one where it is not. These correspond roughly (but not exactly) to conditions of relatively short and long horizontal coherence scales, and to conditions of large and small array gain degradation.

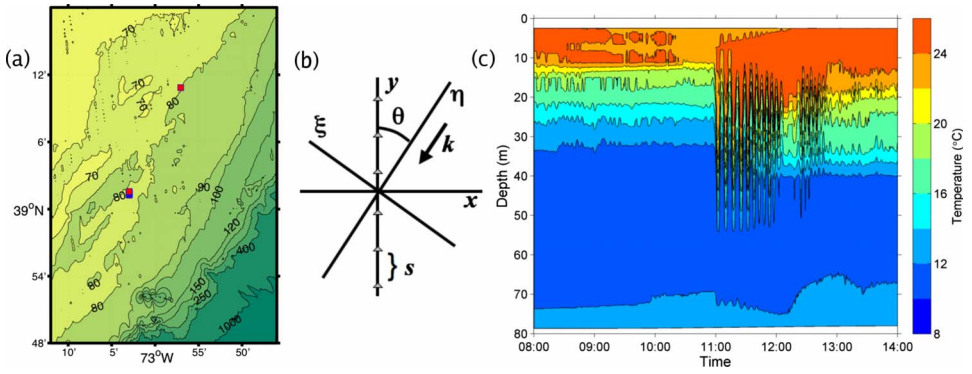

Fig. 1. (Color online) (a) Depiction of the receiver array (southern red dot) and source (northern red dot) moorings. The horizontal leg of the array is aligned very close to north/south. The bearing to the sound source is approximately 26.2° at the southern (VLA) end of the array. (b) Plane view defining acoustic angle of incidence and axis orientations. (c) Contour plot of isotherms measured by a mooring near the acoustic source. Contour intervals are 1.5 C.

2. Data and methods

Data from a 48-element L-array deployed during the Shallow-Water 2006 (SW06) field program[2] are used here to measure coherence. As part of the experiment, numerous acoustic and oceanographic moorings were deployed, with the majority following a "T" shaped geometry. The upright leg of the T had an along-shelf alignment following (approximately) the 80 m isobath, at heading 30° (true), whereas the other was across shelf from depths of 58–500 m (true heading 300°). The L-array was located near the intersection of the T [Fig. 1(a)] and had two sections: A 16-element VLA spanning four-fifths of the water column (water depth 79 m) and a 32-element HLA, 472 m in length, aligned south to north. Moored acoustic sources were placed near the far end of the along-shelf line and near the inshore end of the cross-shelf line, to provide known signals.

The signals considered here are 100 Hz pulses produced by the "Miami Sound Machine" source, located 19.2 km from the L-array [Fig. 1(a)]. The heading from the HLA center to the source was 26.2° [incidence 63.8° from broadside, Fig. 1(b)]. Each half hour the source emitted a continuous series of broadband phase-coded pulses at a center frequency of 100 Hz (90 s, 36 pulses), then switched to higher frequencies. The received signals were replica correlated[3] to create the data shown here. Internal ocean state was measured with moored current meters and thermometers at locations near the source, the receiver, and midway between.

2.1 Synthesized and measured horizontal fields

The emphasis of our technique is to evaluate horizontal coherence in planes transverse to the acoustic propagation direction. This variability can be measured directly with an HLA only for signals at broadside incidence, a limiting geometry for experimental purposes. Here, VLA data are incorporated into the analysis to account for expected range variability of obliquely incident HLA signals.

For this analysis, a synthetic acoustic field is computed from the modal decomposition of each pulse measured along the VLA, and used as a metric for comparison with the data. This procedure separates two spatial decoherence effects. The first effect is caused by mode interference, which degrades coherence if the modes are not fully separated via dispersion and incidence is not broadside. This limits coherence of signals sampled along the array in a manner that is dependent on incident angle. The second effect is caused by azimuthally dependent propagation from the source, which would be evident when the projected array aperture normal to the source direction is large compared to the coherence length in the transverse plane (normal to propagation direction).

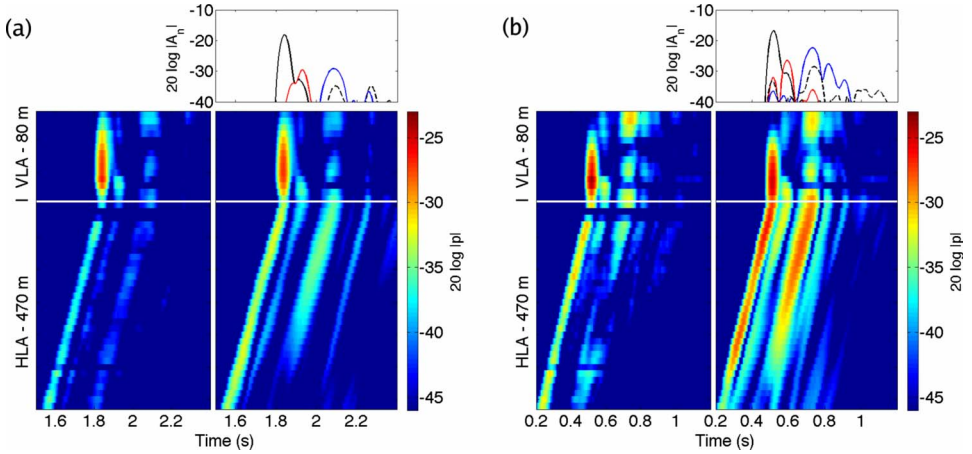

Fig. 2. (Color online) Intensity (measured and synthesized) and mode coefficients along the L-array during different regimes of internal wave activity. The result of the modal decomposition is shown above the synthesized field. (a) Weak scattering period. (b) Strong scattering period.

First, the data are match-filter processed to obtain the complex acoustic pressure, $p_d(\mathbf{r_j},t)$, $\mathbf{r_j}=(x_j,y_j,z_j)$, at each element ($j$) along the L array (the subscript d denotes measured data). Sound speed profiles are determined using temperature data collected along the VLA, and a nearby buoy for the near surface. From these, time-dependent normal mode functions and associated wave number values are determined using a simplified geoacoustic model (discussed below) of the site. Mode filtering is applied to p_d along the VLA to obtain time series of mode content. The acoustic signal at the VLA element positions can be written in terms of normal modes, $p_d(x_0,y_0,z,t)=\Sigma_{n=1}^{N}A_n(t)\phi_n(z,t)$ where p_d is the complex matched-filter output, A_n are the mode coefficients, ϕ_n are the vertical mode functions, and x_0, y_0 locate the VLA at the origin. There are 16 VLA hydrophones and at 100 Hz only 4–6 modes are expected to arrive. Because this system is well determined, the pseudoinverse method[4] is used to obtain the A_n. A 9-layer bottom model is used in the mode computations, in which geoacoustic and stratigraphic properties have been based on past studies conducted at the experimental site.

Assuming the ocean does not change over the horizontal extent of the HLA, the mode wave numbers, amplitudes, and relative mode-shape amplitudes at the seafloor can then be used to synthesize the fixed-mode field along the bottom-resting HLA (or anywhere else). The synthesized field along the HLA is given by

$$p_S(x_0,y-y_0,z_b,t)=\sum_{n=1}^{N}A_n(t)\phi_n(z_b,t)e^{ik_n\Delta\eta}, \tag{1}$$

where the η direction in an (η,ξ) coordinate system is toward the source [Fig. 1(b)] and the subscript S denotes synthetic data. Because the HLA is defined to extend in the y-direction (north in this case), $\Delta\eta=\cos\theta(y-y_0)$, where incident angle θ is defined in Fig. 1(b), and where $z=z_b$ is the seafloor depth.

Figure 2 shows measured and synthesized intensity time series during times of weak and strong scattering effects. The times are 08:30 and 13:30 and the sound speed condition measured at those times can be deduced from Fig. 1(c). In each of Figs. 2(a) and 2(b), the measured intensity is shown on the left, four extracted mode coefficient series $A_n(t)$ are shown above, and to the right is $P_S(t)$ computed using a four-term modal sum. The synthetic fields show expected nonbroadside interference patterns for the fixed-mode situation. For the weakly scattered case [Fig. 2(a)], modes one to four are largely temporally dispersed and resolvable, and the synthetic and measured fields agree for the low modes but differ from each other for the

higher-order, 3rd and 4th modes. For the strong scattering case [Fig. 2(b)], the mode arrivals are multiple and extended (spread) in time, and the fields along the HLA differ strongly from each other.

2.2 Coherence lengths

The field p_d will possess a characteristic scale L_d along the array, defined as the point where coherence (normalized spatially lagged cross-correlation)

$$R_d(\delta) = \mathrm{Re}\left\{ \left\langle \left\langle \frac{P_d(y) \circ P_d^*(y+\delta)}{\left(\sum_t |P_d(y)|^2 \sum_t |P_d(y+\delta)|^2 \right)^{1/2}} \right\rangle_A \right\rangle_E \right\} \tag{2}$$

is reduced to some specified fraction of its zero-lag ($\delta=0$) value, where the brackets $\langle\cdot\rangle_E$ indicate ensemble averaging (in this case averaging over many pulse arrivals), the brackets $\langle\cdot\rangle_A$ indicate averaging along the length of the array (varying y), the $\circ$ denotes the Hadamard (element by element) product, and $P_d(y)$ is the time series $p_d(y,t)$. The time series is of 0.5 s duration. Only the zero time-lag value of a two-dimensional correlation is used, with p_d adjusted to arrive at time zero at each element (beam steering). The nonlinear shape (distortion) of the array, obtained via analysis of fully time dispersed normal modes, is accounted for, with the measured distortion projected onto the $\theta \approx 26.2°$ beam angle causing phase errors of up to 2 radians. The coherence scale L_S of the synthetic field is similarly obtained via $R_S(\delta)$, which is defined analogously to R_d except that p_S is used in place of p_d. Comparing L_d to L_S allows detection of signal fluctuations with smaller coherence scales than resulting from modal interference in the synthetic (fixed A_n and k_n) field. This would indicate azimuthally dependent propagation. Comparing the synthetic and data fields for these situations may divulge the responsible scattering effects.

Array gain calculations can also be used to estimate effective coherence lengths.[5] Under the assumption that noise is uncorrelated between the sensors, the gain degradation can be related to signal coherence length. Signal gain G_c is calculated as

$$G_c(M) = \frac{S^2}{N^2}, \quad S = \left\langle \overline{\frac{1}{M}\sum_{j=M} p_j(t)} \right\rangle_{\mathrm{sa}}, \quad N = \left\langle \overline{\frac{1}{M}\sum_{j=M} p_j(t+\Delta t)} \right\rangle_{\mathrm{sa}}, \tag{3}$$

where $\langle\rangle_{\mathrm{sa}}$ denotes an ensemble average over independent sub-apertures, and the overbar indicates an arithmetic mean in time over the duration of the pulse, S is the received signal, N is the background noise, Δt is a time chosen such that the p_j do not include signal, and $M=2^n$ where $n=0$ to 5 is the number of elements in six HLA subaperture sizes. The time series t for both S and N calculations is of 0.4 s duration.

Theoretical $G_c(M)$ curves can be computed for fields with specific coherence properties and uncorrelated noise. Using the notation of Refs. 5 and 6, let the correlation function be $R(ns)=\rho^n=\exp(-(\alpha n s/\lambda)^p)$, with s being the inter-sensor distance, n a positive integer, λ the acoustic wavelength, α a parameter, and the exponent $p=1$. Computed values of $G_c(M,\rho) = (1+\rho)/(1-\rho) - (2\rho(1-\rho^M))/(M(1-\rho)^2)$ for various ρ (and thus various α) under these assumptions are presented in Figs. 3(a) and 3(b) (smooth curves).[6] Note that a characteristic coherence length is given by $L_h=\lambda/\alpha$, which is easily obtained from ρ. Also note that using a different exponent p will result in analogously different characteristic coherence lengths.

3. Results

Applying the new technique, coherence properties of transmissions from three 6 hour time periods are computed and shown here. The time periods are depicted in Fig. 3(c) which shows symbols at the arrival times of analyzed pulses, along with the signal to noise ratio of the pulses. The pulses are divided into two groups, those with strong p_d, p_S and $R_d(\delta), R_S(\delta)$ similarities (case 1), showing behavior as in Fig. 2(a), and those without, as in Fig. 2(b) (case 2). Also shown

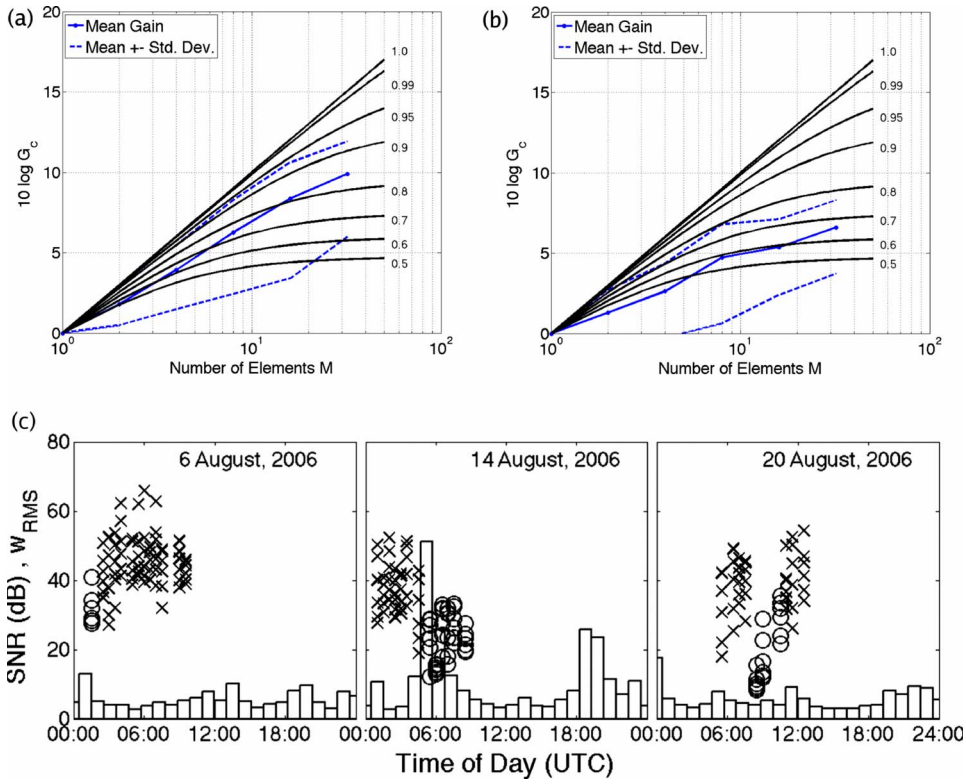

Fig. 3. (Color online) (a) and (b) Array signal gain for the measured data calculated using an ensemble average as a function of aperture size, . (a) Weak scattering time periods. (b) Strong scattering time periods. (c) Plots showing signal to noise ratios for the acoustic transmissions considered in the limiting case coherence plots. Short coherence lengths are indicated by circles and long coherence lengths by x's. Superimposed on the the plot are scaled (20 times), hourly averaged values for the RMS vertical velocity (cm/s).

in Fig. 3(c) are RMS vertical velocity values (scaled by a factor of 20) at one mooring near the HLA, averaged over 1 hour time windows, indicating internal ocean activity, which exhibits some correlation with both the signal to noise ratio and the scattering categorization. Figure 4 shows the correlation functions R_S and R_d for each of the cases, obtained by averaging the correlation functions for individual pulse arrivals.

For the case 1 data, the R curves are consistent with interference patterns of fixed-mode fields. For the case 2 data, the coherence scale from the R_d curve is reduced below that of the R_S via azimuthally dependent propagation and scattering effects. From the curves, correlation scales are defined by where they reach e^{-1} (noting that they can remain high by effects such as coherence in the noise field, for example). For case 1, L_S=220 and L_d=250 m, giving good agreement. For case 2, L_S=140 and L_d=80 m.

Returning to Figs. 3(a) and 3(b), these show $G_c(M)$ computed from the data. The curves show mean results for pulses (plotted with plus/minus one standard deviation) in each of the two groups. The curves can be used to infer ρ and L_h values. These correspond to ρ=0.9, L_h=150 m (case 1 period), and to ρ=0.8, L_h=60 m. Note that there is a mismatch in the array gain degradation curves between the actual theoretical shape and the shape obtained from the data. Possible explanations for this mismatch are that the function $\exp(-ns/H\lambda)$ may be too simple for this data or that an aspect of the data is nonstationary over the ensemble. Because the shapes of the curves do not exactly match, the asymptotic value of each array gain curve is used to obtain ρ (as opposed to selecting ρ from a theoretical curve that is close to the data curve).

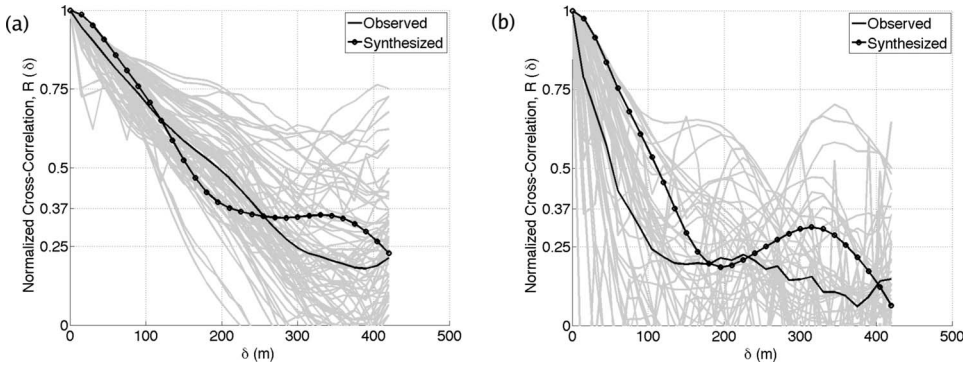

Fig. 4. Relative acoustic coherence along the horizontal line array during the limiting case times. The measured acoustic field (solid curve) is compared against the synthesized field (solid dotted curve). The curves are taken to be the average of individual transmissions (displayed in gray in the plot). (a) Long coherence length (weak scattering) time periods. (b) Short coherence length (strong scattering) time periods.

4. Summary

A method to investigate horizontal coherence of acoustic fields consisting of many normal modes arriving at an L array with nonbroadside geometry has been presented here and applied to a measured data set. The method allows interference of a homogeneous mode structure to be distinguished from horizontal de-correlation from azimuthally varying adiabatic or coupled mode propagation. Coherence length (L_h) results agree with results from array-gain degradation analysis. In addition to providing L_h estimates for given signal incidence angle, the method detects signatures of scattering behavior that can limit array effectiveness at broadside incidence.

Broadband 100 Hz signals along a fixed path during time periods having weak internal variability were observed to have clearly separated modal arrivals and negligible mode multipath effects. In contrast, signals during a period having strong internal variability divulged strong scattering effects and spread-out, multiple mode arrivals. During the period of weak internal ocean activity, L_h was of order 15λ, with estimates from the HLA data and from a synthesized fixed-mode field agreeing. This implies that mode interference sets the horizontal correlation scale, and that the scale will be dependent on incident angle (equivalently, to the source-receiver range difference over the HLA). For our particular geometry, interference controls L_h, so that adjustment to a more-broadside alignment will increase the coherence scale along the array until a limit (not known from this processing) is reached. During the period of strong internal ocean activity, L_h was observed to be shorter, 5λ for the data and 10λ for the synthetic result, consistent with expectations. The shorter result for the data implies that azimuthally varying propagation can degrade array performance. The useful (coherent) aperture for even broadside geometry would be limited, in this case to the projection of the data result onto a plane transverse to the propagation path (i.e., $5\lambda \cos(26.2°) \approx 4.5\lambda$).

Thus, two shallow-water propagation regimes are observed: One where near-broadside HLA geometry may have very long horizontal coherence length and high array gain, and one where it cannot. These analyses will be extended to the entire month-long time series of signals at other frequencies, including those traveling cross shelf. The effect on the results of finite noise level and noise correlation along the array must also be evaluated.

Acknowledgments

The authors acknowledge the use of array processing codes written by Arthur Newhall and Ying-Tsong Lin. We thank Hien B. Nguyen for helping with analysis of signals from the Miami

source. This work was funded by grants to Boston University and the Woods Hole Oceanographic Institution from the Ocean Acoustics Program at the U.S. Office of Naval Research, including an ONR Postdoctoral Fellowship award to the first author.

References and links

[1]M. H. Orr, B. H. Pasewark, S. N. Wolf, J. F. Lynch, T. Schroeder, and C.-S. Chiu, "South China Sea internal tide/internal waves - Impact on the temporal variability of horizontal array gain at 276 Hz," IEEE J. Ocean. Eng. **29**, 1292–1307 (2004).

[2]A. E. Newhall, T. F. Duda, K. von der Heydt, J. D. Irish, J. N. Kemp, S. A. Lerner, S. P. Liberatore, Y.-T. Lin, J. F. Lynch, A. R. Maffei, A. K. Morozov, and A. Shmelev, "Acoustic and oceanographic observations and configuration information for the WHOI moorings from the SW06 experiment," Woods Hole Oceanographic Institution, WHOI Tech. Report No. WHOI-2007-04, Woods Hole, MA, 2007.

[3]H. DeFerrari, N. Williams, and H. Nguyen, "Focused arrivals in shallow water propagation in the Straits of Florida," ARLO **4**, 106–111 (2003).

[4]C. T. Tindle, K. M. Guthrie, G. E. J. Bold, M. D. Johns, D. Jones, K. O. Dixon, and T. G. Birdsall, "Measurements of the frequency dependence of normal modes," J. Acoust. Soc. Am. **64**, 1178–1185 (1978).

[5]W. M. Carey, "The determiniation of signal coherence length based on signal coherence and gain measurements in deep and shallow water," J. Acoust. Soc. Am. **104**, 831–837 (1998).

[6]H. Cox, "Line array performance when the signal coherence is spatially dependent," J. Acoust. Soc. Am. **54**, 1743–1746 (1973).